Two-dimensional nuclear magnetic resonance study of phason and amplitudon relaxation mechanisms in structurally incommensurate Rb_2ZnCl_4

1992 J. Phys.: Condens. Matter 4 7203

(http://iopscience.iop.org/0953-8984/4/35/006)

J. Phys.: Condens. Matter 4 (1992) 7203–7218. Printed in the UK

Two-dimensional nuclear magnetic resonance study of phason and amplitudon relaxation mechanisms in structurally incommensurate Rb_2ZnCl_4

J Dolinšek, T Apih and R Blinc

Jozef Stefan Institute, University of Ljubljana, Jamova 39, 61 111 Ljubljana, Slovenia

Received 6 August 1991, in final form 14 February 1992

Abstract. In structurally incommensurate systems phason and amplitudon thermal fluctuations of the frozen-in modulation wave provide for two different nuclear magnetic resonance (NMR) spin–lattice relaxation mechanisms. These two relaxation mechanisms influence different parts of the inhomogeneously broadened NMR absorption spectrum differently. They can be resolved in principle by a conventional one-dimensional measurement of the spin–lattice relaxation time T_1 over the NMR lineshape. Here we show that a two-dimensional NMR spin–lattice relaxation technique provides a very convenient way of determining the variation of T_1 over the lineshape by the use of normalized contour plots. The results for the central transition of ^{87}Rb in Rb_2ZnCl_4 show that the measured phason-induced spin–lattice relaxation time is temperature-independent. The much less efficient amplitudon relaxation mechanism is bypassed in part by the cross-relaxation process of the amplitudon-relaxed parts to the phason-relaxed parts of the NMR lineshape. The theoretical prediction for the total variation of T_1 over the lineshape for the cross-relaxation process agrees with the experimental value of 3.

1. Introduction

Structurally incommensurate (INC) systems are characterized by the modulation of some local atomic property, which varies in space in such a way that its periodicity is an irrational fraction of the periodicity of the host lattice. The modulation is a result of an instability of the high-temperature phase against a soft mode with a critical wavevector q_I, which is shifted by a small amount from a commensurate value q_C,

$$q_I = q_C(1 - \Delta) \qquad \Delta \ll 1 \tag{1}$$

where Δ is temperature-dependent. With decreasing temperature, Δ tends to zero and the lost translational periodicity is recovered at the 'lock-in' transition (Bruce and Cowley 1978), where the crystal again becomes commensurate (C).

The frozen-in incommensurate modulation wave is not completely static, but undergoes thermal fluctuations in phase and amplitude. In the plane-wave limit, where the wavelength of the modulation wave is much longer than the interatomic distances, a one-dimensional modulation wave can be described by a displacement u

$$u(x,t) = A(t)e^{i\phi(x,t)}. \tag{2}$$

0953-8984/92/357203+16$04.50

The excitation spectrum (figure 1) consists of two modes (Žumer and Blinc 1981). The first is the amplitudon branch and corresponds to oscillations of the amplitude of the displacement, $A(t) = A_0 + \delta A(t)$, and behaves like an 'optic-like' phonon. The dispersion relation is

$$\omega_{Ak}^2 = 2a(T_I - T) + Kk^2 \tag{3}$$

where a = constant and $k = q - q_I$. The second is the 'acoustic-like' phason branch, which corresponds to oscillations of the phase of the modulation wave, $\phi(x,t) = \phi_0(x) + \delta\phi(x,t)$, with the dispersion relation

$$\omega_{\phi k}^2 = \Delta_\phi^2 + Kk^2. \tag{4}$$

Here Δ_ϕ represents the phason gap (Bruce and Cowley 1978, Bruce 1980, Blinc *et al* 1985a, 1986), induced by the pinning of the modulation wave to impurities and by the discrete lattice and commensurability effects. In the strong pinning limit (Blinc *et al* 1986), which should hold for the nominally pure crystals, the phason gap is expected to be temperature-independent, $\Delta_\phi \neq f(T)$. This is in contrast to the amplitudon gap (the first term on the right-hand side of (3)), which for $k = 0$ depends on temperature as $\Delta_A \propto (T_I - T)^{1/2}$.

In nuclear magnetic resonance (NMR) the phason and amplitudon excitations represent two kinds of relaxation mechanisms in the INC phase for nuclei with non-zero electric quadrupole moment (Žumer and Blinc 1981). The phason branch is very effective in the relaxation process since its frequencies can come in the range of the nuclear Larmor frequency, thus providing a strong relaxation mechanism. In an ideal INC phase with no defects, the phason frequencies would even become equal to zero, reflecting the fact that the energy of an INC system is independent of the phase of the modulation wave. In a real crystal, dislocations and other types of impurities induce a finite phason gap, which in Rb_2ZnCl_4 has been estimated (Blinc *et al* 1985a) to be of the order 10^{11} s^{-1}. Phason-induced spin–lattice relaxation time $T_{1\phi}$ is directly proportional to the phason gap (Blinc *et al* 1985a) and thus temperature-independent,

$$T_{1\phi}^{-1} = C\Gamma_\phi/\Delta_\phi. \tag{5}$$

Here Γ_ϕ is the phason damping constant. The amplitudon-induced spin–lattice relaxation time, on the other hand, reflects the temperature-dependent energy gap Δ_A in the amplitudon spectrum,

$$T_{1A}^{-1} = C\Gamma_A/\Delta_A \tag{6}$$

where $\Delta_A = [2a(T_I - T)]^{1/2}$ in the mean-field approximation and Γ_A is the amplitudon damping constant. Δ_A is of the order of a phonon frequency at temperatures different from the paraelectric–INC transition temperature T_I.

The technique for the separation of phason and amplitudon contributions to the spin–lattice relaxation rate for quadrupolar nuclei (Žumer and Blinc 1981, Blinc *et al* 1985a, b) consists of measuring the variation of spin–lattice relaxation time over the inhomogeneous frequency distribution. This distribution is an inhomogeneously broadened absorption spectrum limited by two edge singularities. It directly reflects the spatial variation of the modulation wave since it modulates the local electric field gradient (EFG) and thus the electric quadrupole interaction of nuclei, lying on the

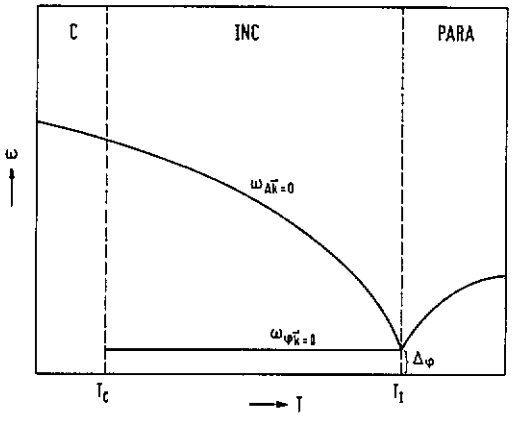

Figure 1. A schematic representation of the temperature dependence of the incommensurate soft mode, the amplitudon and the phason.

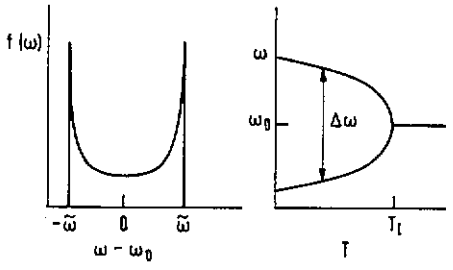

Figure 2. Static incommensurate NMR lineshape $f(\omega)$ and temperature dependence of splitting of the edge singularities $\Delta\omega$ for a linear expansion of frequency versus displacement.

modulation wave. Each element of the EFG tensor at a particular nuclear site can be expanded in powers of the nuclear displacements $u(x)$ from the positions in the paraelectric unit cell. The quadrupole perturbed nuclear resonance frequency of a given nucleus ω can also be expanded in powers of the displacements around the paraelectric value ω_0,

$$\omega = \omega_0 + au(x) + \cdots. \tag{7}$$

The frequency distribution function, which determines the NMR lineshape, is in the constant-amplitude approximation (Blinc 1981) for the static case given by (Blinc *et al* 1985b)

$$f(\omega) = \frac{\text{constant}}{|\mathrm{d}\omega/\mathrm{d}x|}. \tag{8}$$

By taking only the linear term in the expansion (7), replacing $u(x)$ with $u(x) = A\cos\phi(x)$ and defining $\tilde{\omega} = aA$, we get for $f(\omega)$

$$f(\omega) = \frac{\text{constant}}{\{1 - [(\omega - \omega_0)/\tilde{\omega}]^2\}^{1/2}}. \tag{9}$$

$f(\omega)$ exhibits two edge singularities at $\omega = \pm\tilde{\omega}$ (figure 2). The splitting between the singularities increases with temperature as $\Delta\omega = 2\tilde{\omega} \propto A \propto (\Delta T)^{\beta}$. The measured NMR lineshape is a convolution of the frequency distribution function $f(\omega)$ with the homogeneous lineshape $L(\omega)$,

$$F(\omega) = \int_{-\infty}^{\infty} f(\omega_c) L(\omega - \omega_c)\,\mathrm{d}\omega_c. \tag{10}$$

The intensities of the edge singularities come from the nuclei that lie in the vicinity of the extrema of the modulation wave. The nuclei that lie in the region where the

amplitude of the modulation wave is small contribute to the intensity in the middle of the spectrum. These two different 'types' of nuclei have different relaxation mechanisms. The nuclei near the extrema of the modulation wave lie in the region where the amplitude fluctuations are large and are thus relaxed mainly via amplitudons. The nuclei that lie far away from the extrema, where the amplitude is small, experience mainly phason fluctuations and are thus relaxed by phasons. Measuring the effective spin–lattice relaxation rate over the inhomogeneous frequency distribution thus enables one in principle to determine separately the phason and amplitudon relaxation contributions. In the simplest case, when we assume a local relation (Blinc 1981) between the resonance frequency and the displacement, $\omega_i = \omega(u(x_i))$, and neglect the contributions to the frequency shift from nuclei at positions other than x_i, we get for the effective spin–lattice relaxation rate (Blinc *et al* 1985b)

$$\frac{1}{T_1} = X^2 \frac{1}{T_{1A}} + (1 - X^2) \frac{1}{T_{1\phi}}. \tag{11}$$

Here $X = \cos\phi(x) = (\omega - \omega_0)/\tilde{\omega}$ represents the normalized frequency. Expression (11) enables one to extract the phason $T_{1\phi}$ and T_{1A} contributions from the analysis of the variation of the spin–lattice relaxation time over the inhomogeneous lineshape (equation (9)). At the edge singularities $X = \pm 1$ one expects to get the pure amplitudon contribution T_{1A}, which is temperature-dependent as

$$T_{1A}^{-1} \propto 1/(T_I - T)^{1/2} \tag{12}$$

in the mean-field approximation. In the centre of the spectrum where $X = 0$, on the other hand, one gets the pure phason contribution, which is independent of temperature and directly proportional to the phason gap,

$$T_{1\phi}^{-1} \propto 1/\Delta_\phi \neq f(T). \tag{13}$$

By lowering the temperature through the incommensurate–commensurate transition T_c the phason relaxation time $T_{1\phi}$ should jump discontinuously to a much larger value, which expresses the fact that there are no longer phasons in the commensurate phase. The amplitudon relaxation time T_{1A} should, however, grow continuously throughout the whole INC phase and match continuously the commensurate value (figure 1).

In our previous experiments on Rb_2ZnCl_4 (Blinc *et al* 1986) and $[N(CH_3)_4]_2ZnCl_4$ (Blinc *et al* 1985a) an attempt was made to resolve experimentally T_{1A} and $T_{1\phi}$ via equations (11) and (9). The analysis of variation of the effective T_1 over the lineshape behaved qualitatively correctly. T_1 was the shortest in the middle of the spectrum. This contribution was also temperature-independent, so that we believe that we measured the phason contribution $T_{1\phi}$ correctly. The T_1 value measured on the edge singularities was slightly longer than $T_{1\phi}$. The difference was, however, only a factor of about 2, which is much smaller than expected from the phason–amplitudon picture. It was also temperature-independent, except in the vicinity of the para–INC transition temperature T_I, where it showed a critical dependence proportional to $(T_I - T)^\beta$. Both contributions are shown for Rb_2ZnCl_4 in figure 3. The small difference between the two relaxation times and the temperature independence of the relaxation time, measured at the singularities, show that this relaxation contribution does not

behave like the theoretically predicted amplitudon contribution T_{1A}. T_{1A} should grow continuously throughout the INC phase and smoothly match the T_1 value of the commensurate phase at T_c. We thus believe that the relaxation time thus determined is not the pure T_{1A} contribution. Similar results were found in $[N(CH_3)_4]_2ZnCl_4$. The measurements were made with the inversion recovery technique. The pulse sequence used was a three-pulse π–Δ–$\pi/2$–τ–π–τ–t sequence with a $\pi/2$ pulse length of 5 μs. Here the last two pulses form an echo to overcome the receiver dead-time problems and Δ is the relaxation delay. Some 20 relaxation delays were taken, the longest delay being about $5T_1$. No phase cycling procedure to compensate the pulse errors was applied to the above sequence. Further analysis of the experimental data to extract the T_1 values was made by a simple 'ruler and eye' technique on semi-log paper. This accounts for the discrepancy by a factor of about 2 in the $T_{1\phi}$ values determined from these early measurements and the more precise ones to be described below.

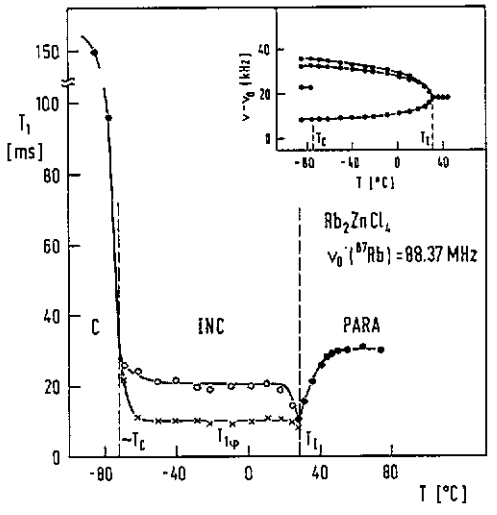

Figure 3. Temperature dependence of spin–lattice relaxation time T_1, measured on the central transition $1/2 \rightarrow -1/2$ of ^{87}Rb in Rb_2ZnCl_4 at an orientation $a \perp H_0$, $\angle(c, H_0) = 122°$. In the INC phase crosses represent the phason contribution $T_{1\phi}$ and open circles represent T_1, measured at the edge singularities, where the amplitudon relaxation is expected to be dominant. The inset shows the temperature dependence of splitting of the edge singularities.

To elucidate the question of why we do not get the amplitudon contribution correctly, we decided to make a high-resolution two-dimensional spin–lattice relaxation study of ^{87}Rb in Rb_2ZnCl_4. The use of normalized two-dimensional (2D) contour plots provides an extremely sensitive way to determine, and a convenient way to display, the variation of spin–lattice relaxation time over the absorption spectrum. This 2D technique will be described in the next section.

2. Two-dimensional spin–lattice relaxation in incommensurate systems

The use of a 2D relaxation technique with normalized contour plots (Millhauser and Freed 1984) has been applied to deuterons ($I = 1$) in liquid-crystalline polymers (Schleicher *et al* 1989, 1990, Müller *et al* 1990). The name 'two-dimensional relaxation' is somewhat misleading, since this is not a two-dimensional NMR experiment in the usual sense. There we look for the absorption of the spin system as a function of two frequency variables. In a two-dimensional relaxation experiment, only one

dimension shows the absorption as a function of a frequency variable, whereas the second dimension shows the Fourier transform of a magnetization recovery curve.

In the 2D spin–lattice relaxation technique, applied to incommensurate systems, one tries to get the variation of the spin–lattice relaxation time T_1 over the inhomogeneously broadened absorption spectrum. $T_1 = T_1(u)$ depends on the displacement u of the given nucleus on the modulation wave. At the beginning of the pulse sequence we prepare the spin system in a non-equilibrium state, e.g. we invert the population with a single π pulse. The system then relaxes towards equilibrium in the evolution period t_1,

$$\frac{\partial \rho}{\partial t_1} = -\frac{1}{T_1(u)}(\rho - \rho_{eq}) \tag{14}$$

where ρ is the density operator. The solution at time $t = t_1$ is

$$\rho(t_1) = \rho_{eq} + [\rho(0) - \rho_{eq}] \exp[-t_1/T_1(u)]. \tag{15}$$

The amplitude of the signal at the beginning of the detection period will be for $\rho(0) = -I_0$

$$A(t_1, u) = I_0\{1 - 2\exp[-t_1/T_1(u)]\}. \tag{16}$$

At the end of the evolution period we apply a 'read' $\pi/2$ pulse and observe in the detection period t_2 the normal free induction decay (FID). For $I > 1/2$ this is a quadrupole-perturbed Zeeman signal. The signal can be written as

$$S(t_1, t_2, u) = A(t_1, u)g(t_2). \tag{17a}$$

Here $g(t_2)$ represents the signal of all nuclei with distributed resonance frequencies $\omega = \omega_0 + \tilde{\omega}X$. Here $X = \cos\phi(x)$ lies in the interval $[-1, 1]$. The probability distribution $G(X)$ is obtained from the equation $G(X)\,dX = n(x)\,dx = \text{constant}\,dx$, where $n(x)$ represents a constant density of nuclei along the modulation wave. The signal $g(t_2)$ can be written as

$$g(t_2) = \int_{-1}^{1} \exp[i(\omega_0 + \tilde{\omega}X)t_2] \exp(-t_2/T_2) \frac{dX}{(1 - X^2)^{1/2}}. \tag{17b}$$

First we make a Fourier transform over the t_2 variable and get

$$S(t_1, \omega_2, u) = A(t_1, u)F(\omega_2) \tag{18}$$

where $F(\omega_2)$ is given by equation (10). Then we subtract the spectrum $S(t_1 = \infty, \omega_2, u)$ from the signal (18) and get

$$S(t_1, \omega_2, u) = K \exp[-t_1/T_1(u)] \frac{1}{\{1 - [(\omega_2 - \omega_0)/\tilde{\omega}]^2\}^{1/2}}. \tag{19}$$

Here we took for simplicity an infinitely sharp homogeneous lineshape $L(\omega)$, thus making $F(\omega_2)$ equal to $f(\omega_2)$ (equation (9)). Introducing $X = (\omega_2 - \omega_0)/\tilde{\omega}$, we make the second Fourier transform over the t_1 variable and get for the real part

$$S(\omega_1, X, u) = \frac{1/T_1(u)}{\omega_1^2 + [1/T_1(u)]^2} \frac{1}{(1 - X^2)^{1/2}}. \tag{20}$$

Since $T_1(u)$ is a function of X via $u = A\cos\phi(x) = AX$ (equation (11)) we get finally

$$S(\omega_1, X) = \frac{X^2/T_{1A} + (1-X^2)/T_{1\phi}}{\omega_1^2 + [X^2/T_{1A} + (1-X^2)/T_{1\phi}]^2} \frac{1}{(1-X^2)^{1/2}}. \tag{21}$$

Equation (21) shows that the lineshape in the ω_1 domain is a Lorentzian with a half width at half height (HWHH) $1/T_{1\phi}$ at the centre of the spectrum $X = 0$ and HWHH $1/T_{1A}$ at the edge singularities $X = \pm 1$.

In a real experiment, performed on the central transition $1/2 \rightarrow -1/2$ of $^{87}Rb(I = 3/2)$ nuclei, we used a three-pulse sequence π–t_1–$\pi/2$–τ–π–τ–t_2, where the second and third pulses form an echo sequence to overcome the receiver dead-time problems. The detection period t_2 thus starts at the top of the echo. The $\pi/2$ pulse length was 5 μs. A suitable phase cycling was used to minimize the pulse errors. The first π pulse was cycled in steps $+X$ and $-X$ and the signals added in order to get the magnetization immediately after the pulse pointing exactly along the $-Z$ direction. The last π pulse was also cycled in steps $+X$ and $-X$ and the signals co-added in order to get rid of the remaining FID after the last pulse. Cyclops phase cycling (Hoult and Richards 1975) was used in addition to minimize the errors of the quadrature detection, so that one complete phase cycle involved 16 steps.

Since the signal is amplitude-modulated only with no phase modulation in the t_1 domain, it is possible to get a pure absorption 2D spectrum by applying a real Fourier transformation to the t_1 domain. The two copies of the absorption spectrum at $\pm\omega_1$ are both centred at $\omega_1 = 0$ and fall exactly on each other, so there is no need to split them by the use of the 'time-proportional phase increments' (TPPI) method (Bodenhausen *et al* 1980). The use of the phase-sensitive, pure absorption 2D spectrum is an essential point in a study of the variation of T_1 over the spectrum, since the 2D spectrum is not distorted as it is in the magnitude or phase-sensitive mixed-phase mode. After both Fourier transformations, a normalized contour plot was made (Millhauser and Freed 1984) by dividing all slices along ω_2 by the centre slice at $\omega_1 = 0$. The centre normalized contour thus becomes a straight line of value 1. The deviation of other contours at $\omega_1 \neq 0$ from the straight lines is a very sensitive tool to observe the variation of T_1 over the absorption line. Here it should be pointed out that this 2D normalized contour plot technique yields in principle no additional or more precise information to what is obtained in a conventional 1D spin–lattice relaxation measurement. It represents a convenient way to display the variation of T_1 over the lineshape. Its high precision is due to the fact that we are using a large number (e.g. 256) of closely spaced relaxation delays, with the longest delay extending up to many (e.g. 25) times the longest relaxation time constant met in the experiment. The high sensitivity is, on the other hand, due to the normalization procedure—division of all slices along ω_2 with the central slice at $\omega_1 = 0$. Such a division is more sensitive to the variation of T_1 over the lineshape.

3. Results and discussion

A 2D spin–lattice relaxation study has been performed on the central transition $1/2 \rightarrow -1/2$ of ^{87}Rb in Rb_2ZnCl_4 at an orientation $a \perp H_0$ and $\angle(c, H_0) = 122°$. The crystallographic axes are taken in a system in which the b axis becomes the

axis of spontaneous polarization below T_c. At this particular orientation it has been shown (Blinc *et al* 1986) from the temperature dependence of splitting of the edge singularities that the expansion of resonance frequency in powers of the displacements (equation (7)) is well described by retaining the linear term only. Such a linear expansion gives the same results (Blinc *et al* 1985b) in the local and non-local approximations. The term 'local approximation' is used for the case when the frequency of a given nucleus depends only on the incommensurate displacement of the resonating nucleus and the displacements of the ions moving in phase with it. This approximation is valid only when the wavelength of the modulation wave is large compared to the size of the region from which comes the dominant contribution to the NMR frequency. When this condition is not fulfilled, the relation between the resonance frequency and the nuclear displacements becomes non-local, i.e. a given nucleus 'sees' in principle all the ions in the crystal. The chosen orientation thus enabled us to treat the problem quite generally. The measurements were performed at three different temperatures. The first was taken at $T = 28\,°C$, which is one degree below the para–incommensurate transition temperature ($T_1 = 29\,°C$). On figure 4(*a*) a 2D contour plot (not normalized) of the spectrum at $T = 28\,°C$ is shown, where the ω_2 domain shows the normal incommensurate lineshape and the ω_1 domain shows the Fourier transform of the magnetization recovery curve. The cross sections $\omega_1 = 0$ and ω_2 at the position of the left edge singularity are shown above and on the left side of the contour plot respectively. The normalized contour plot (the contour plot from figure 4(*a*) with all slices along ω_2 divided by the central slice $\omega_1 = 0$) is shown on figure 4(*b*). Figures 5(*a, b*) and 6(*a, b*) show the corresponding spectra at $T = 13.7\,°C$ and $T = -22\,°C$; the last one already lies in the temperature regime where the plane-wave approximation starts to break down and the description of a soliton wave starts to become appropriate. In all three cases, the number of relaxation delays (number of points sampled in the t_1 domain) was 256, covering the range up to 320 ms, which is around 25 times longer than the longest time constant met in the experiment. On the normalized contour plots the contours are drawn at 100, 85, 70, 55, 40, 25 and 10% of maximum height. The maximum variation of the spin–lattice relaxation time over the lineshape is given by the total span of the contours at certain height in the ω_1 dimension. As can be seen from figures 4(*b*), 5(*b*) and 6(*b*), this variation is the same for all three temperatures. By making a theoretical fit (figure 7) with equation (21) we get the ratio $T_{1A}/T_{1\phi} = 3.01$, so that the relaxation time, measured at the edge singularities, is three times longer than the one in the middle of the spectrum.

So far the experimental data of the variation of relaxation time over the lineshape did not involve any model calculation or *ansatz* for fitting the T_1 curves. We did not even have to know the absolute value of any of the time constants involved. The total variation of T_1 over the lineshape is thus a pure experimental outcome and so the above-described normalized contour plot 2D method can be treated as the 'honest' way for such studies.

The value of $T_{1\phi}$ is found from the linewidth at half height in the ω_1 domain at such an ω_2 position that the normalized contour plot is the broadest. For $T = 28\,°C$ we get $T_{1\phi} = 4.6$ ms, for $T = 13.7\,°C$, $T_{1\phi} = 4.5$ ms and for $T = -22\,°C$, $T_{1\phi} = 4.2$ ms.

These precise measurements thus gave results on the total variation of T_1 over the incommensurate lineshape, which are not much different from the early ones (figure 3), which were obtained by a simpler technique. Two experimental facts are

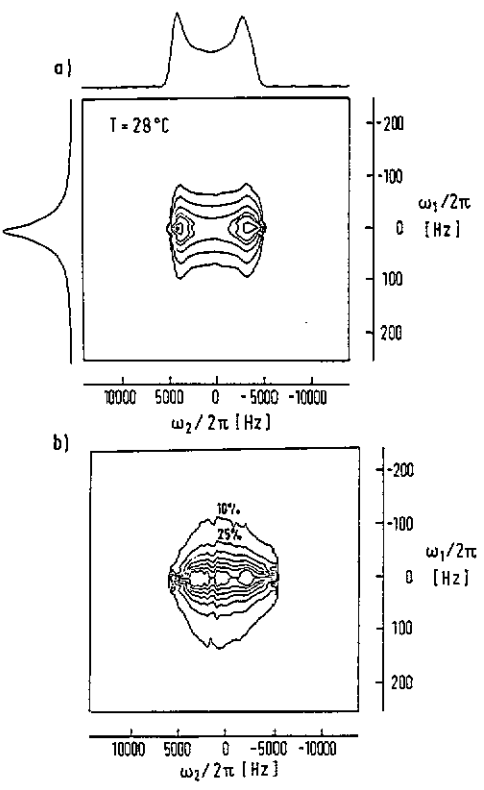

Figure 4. (*a*) A 2D contour plot of ^{87}Rb 'spin–lattice relaxation' spectrum in Rb_2ZnCl_4 at $T = 28$ °C and $\nu_0(^{87}Rb) = 88.34$ MHz. The ω_2 domain shows incommensurate NMR lineshape and the ω_1 domain shows the Fourier transform of the magnetization recovery curve. Cross sections $\omega_1 = 0$ and ω_2 at the position of the edge singularity $\omega_2/2\pi = 3500$ Hz are shown above and on the left side of the contour plot respectively. (*b*) Normalized contour plot at $T = 28$ °C (same plot as above but all cross sections along ω_2 divided by the central cross section $\omega_1 = 0$). Contours are drawn at 100% (centre line), 85, 70, 55, 40, 25 and 10% of maximum height.

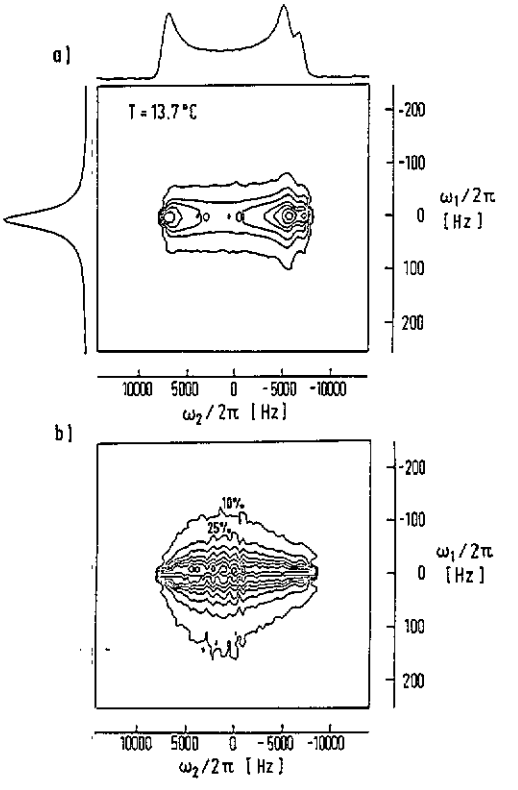

Figure 5. (*a*) A 2D contour plot of ^{87}Rb 'spin–lattice relaxation' spectrum in Rb_2ZnCl_4 at $T = 13.7$ °C and $\nu_0(^{87}Rb) = 88.34$ MHz. The ω_2 domain shows incommensurate lineshape and the ω_1 domain shows the Fourier transform of the magnetization recovery curve. Cross sections $\omega_1 = 0$ and ω_2 at the position of the edge singularity $\omega_2/2\pi = 7000$ Hz are shown above and on the left side of the contour plot respectively. (*b*) Normalized contour plot at $T = 13.7$ °C (same plot as above but all cross sections along ω_2 divided by the central cross section $\omega_1 = 0$). Contour levels are the same as on figure 4(*b*).

now in favour of the statement that, with the method of measuring the variation of T_1 over the lineshape for the quadrupole-perturbed Zeeman lines, we measure the phason relaxation contribution correctly, but we do not measure correctly the amplitudon relaxation contribution. The first fact is that the phason contribution $T_{1\phi}$ is short, temperature-independent and jumps at the INC–commensurate transition to a high value, since the phason mode is no longer present. The second fact is that at the edge singularities we obtain a T_1 that is also temperature-independent and only three times longer than $T_{1\phi}$. This obviously cannot be identified as the amplitudon relaxation time T_{1A}, since T_{1A} would behave as $T_{1A} \propto (T_I - T)^{1/2}$ and go smoothly

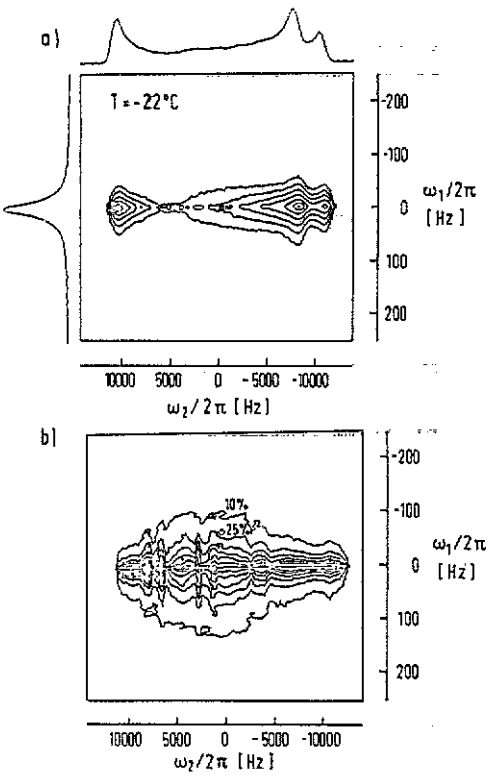

Figure 6. (*a*) A 2D contour plot of ^{87}Rb 'spin–lattice relaxation' spectrum in Rb_2ZnCl_4 at $T = -22$ °C and $\nu_0(^{87}Rb) = 88.34$ MHz. The ω_2 domain shows incommensurate lineshape and the ω_1 domain shows the Fourier transform of the magnetization recovery curve. Cross sections $\omega_1 = 0$ and ω_2 at the position of the edge singularity $\omega_2/2\pi = 10\,000$ Hz are shown above and on the left side of the contour plot respectively. (*b*) Normalized contour plot at $T = -22$ °C (same plot as above but all cross sections along ω_2 divided by the central cross section $\omega_1 = 0$). Contour levels are the same as on figure 4(*b*).

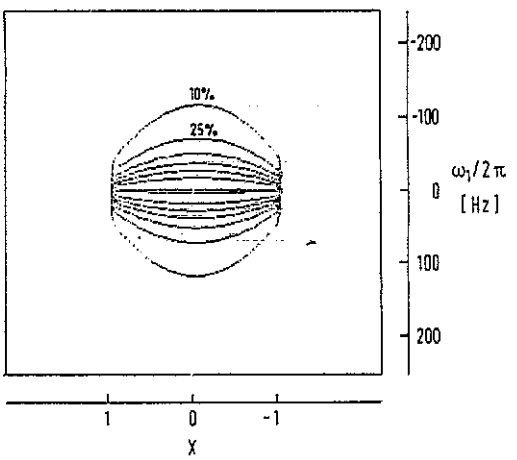

Figure 7. Theoretical normalized contour plot, computed from equation (21) for the ratio $T_{1A}/T_{1\phi} = 3$. Contours are drawn at 100% (centre line), 85, 70, 55, 40, 25 and 10% of maximum height. Here $X = (\omega_2 - \omega_0)/\tilde{\omega}$ is a normalized ω_2 frequency.

through the INC phase to a commensurate value. It is obvious that some other relaxation mechanism bypasses the amplitudon mechanism. This could be explained by the following simplified consideration. If the system of nuclear spins turns out of equilibrium, then those nuclei that see the phason fluctuations relax towards equilibrium with time constant $T_{1\phi}$. Except close to T_I, $T_{1\phi}$ is much shorter than T_{1A}. The nuclei that are relaxed by amplitudon fluctuations see the phason-relaxed nuclei already in thermal equilibrium, i.e. they behave similarly to paramagnetic impurities. The magnetic dipolar coupling between both types of nuclei then transfers the polarization from phason-relaxed to amplitudon-relaxed nuclei in a cross-relaxation process. This bypass relaxation mechanism would imply that the relaxation time of the nuclei, which are supposed to be relaxed nominally by amplitudons, would behave with temperature

in the same way as $T_{1\phi}$ with its value close to $T_{1\phi}$, as is also seen in the experiment. For the cross-relaxation processes to occur frequently, one needs a considerable overlap between the resonance lines of coupled nuclei. To see this in our case, we made a 2D 'separation of interactions' experiment (Dolinšek 1991). Here we get in the ω_2 frequency dimension a normal inhomogeneously broadened INC lineshape. This lineshape is a convolution of a static frequency distribution function $f(\omega)$ (equations (8) and (9)), which describes the distribution of quadrupole-perturbed Zeeman frequencies of isolated nuclei, with the homogeneous lineshape $L(\omega)$ (equation (10)). The homogeneous lineshape $L(\omega)$ is determined by the homonuclear dipolar interaction and is obtained in the ω_1 domain. $L(\omega)$ determines the overlap between nuclei at different positions in the frequency distribution function and determines the efficiency of the cross-relaxation process. Our measurement was made at $T = 16.2$ °C (figure 8). For the inhomogeneous lineshape we found a full width at half height (FWHH) of 13 kHz and for the homogeneous linewidth an FWHH of 500 Hz. Since the frequency distribution function $f(\omega)$ is a continuous function of different resonant frequencies, the above overlap could provide a 'bridge' through all parts of the inhomogeneous lineshape and enables the cross-relaxation process to transfer polarization from the centre of the line towards the edge singularities.

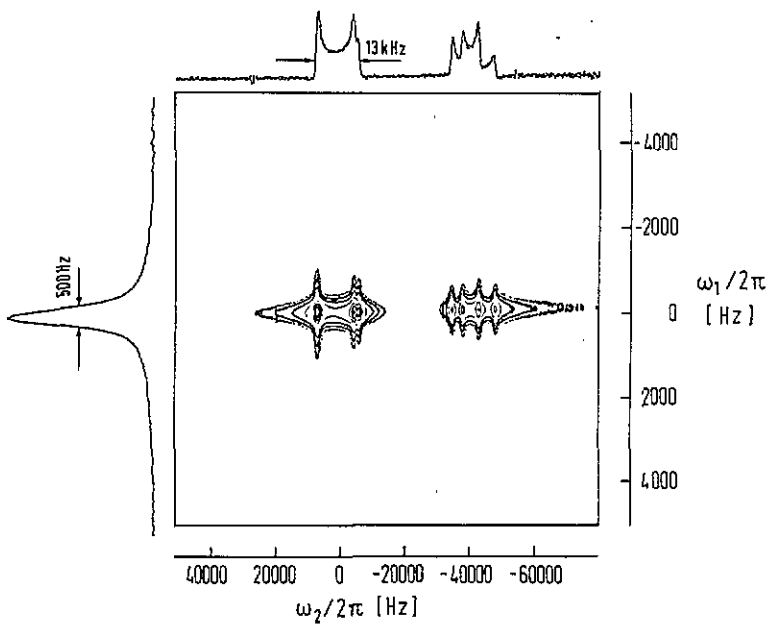

Figure 8. Two-dimensional 'separation of interactions' spectrum of ^{87}Rb $1/2 \rightarrow -1/2$ transition in Rb_2ZnCl_4 at an orientation $a \perp H_0$, $\angle(c, H_0) = 122°$ and $T = 16.2$ °C. The ω_2 domain shows the inhomogeneously broadened incommensurate lineshape and the ω_1 domain shows the homogeneous lineshape, determined by the homonuclear dipolar interaction of Rb nuclei. The projections on both frequency axes are also shown.

A theoretical description of the cross-relaxation phenomenon mentioned above requires first a detailed consideration of the recovery of magnetization towards equilibrium for spin $I = 3/2$ for the case of pure quadrupolar relaxation. This should describe appropriately the pure phason and pure amplitudon relaxations, since it is the EFG tensor that becomes time-dependent by the phason and amplitudon fluctuations.

The energy levels of a quadrupolar nucleus $I = 3/2$ are in general not equidistant and the spin–lattice relaxation cannot be described by a single relaxation rate, but rather by two transition probabilities $W^{(1)}$ and $W^{(2)}$ describing the transitions of the magnetic quantum numbers $\Delta m = \pm 1$ and $\Delta m = \pm 2$ respectively. We write down the kinetic equations describing the time development of the deviations $\Delta\eta_i$ of the level populations η_i defined as $\eta_i = \eta_{i0} + \Delta\eta_i$, where η_{i0} represents the thermal equilibrium population of the ith level. The four kinetic equations (Abragam 1961, Žumer and Blinc 1981) can be solved analytically. When the central transition $1/2 \rightarrow -1/2$ is irradiated only and the $\pm 3/2$ levels stay unperturbed by the RF excitation field, we have the initial conditions after the pulse

$$\eta_{1/2}(t=0) = \eta_{-1/2}(t=0) \qquad \text{(saturation of central transition)}$$

$$\Delta\eta_{\pm 3/2}(t=0) = 0 \qquad \text{(unperturbed } \pm 3/2 \text{ levels)}.$$

For that part of the magnetization that corresponds to $\pm 1/2$ levels only, we get

$$(\eta_{1/2} - \eta_{-1/2})_t - (\eta_{1/2} - \eta_{-1/2})_0 = A[\exp(-2W^{(1)}t) + \exp(-2W^{(2)}t)] \tag{22}$$

where A is a normalization constant. This yields in general a two-exponential magnetization recovery. Only for the case $W^{(1)} \simeq W^{(2)}$ do we get a single-exponential recovery and an effective T_1 can be defined. The two transition probabilities $W^{(1)}$ and $W^{(2)}$ depend strongly on orientation of the crystal with respect to the magnetic field. One can compute $W^{(1)}$ and $W^{(2)}$ from the general theory of relaxation (Slichter 1980). For $W^{(1)}$ one gets

$$W^{(1)} = 12\left(\frac{E}{h}\right)^2 \int_{-\infty}^{\infty} \overline{[\Delta T_{xy}(0)\Delta T_{xy}(t) + \Delta T_{xx}(0)\Delta T_{xx}(t)]} \exp(-i\omega_0 t)\,dt \tag{23}$$

and for $W^{(2)}$

$$W^{(2)} = 12\left(\frac{E}{h}\right)^2 \int_{-\infty}^{\infty} \left\{\tfrac{1}{4}\overline{[\Delta T_{xx}(0)\Delta T_{xx}(t) + \Delta T_{yy}(0)\Delta T_{yy}(t)]} + \overline{\Delta T_{xy}(0)\Delta T_{xy}(t)}\right\} \exp(-2i\omega_0 t)\,dt. \tag{24}$$

Here $E = e^2Q/4I(2I-1)$, T_{ij} denotes an element of the EFG tensor, ω_0 is the nuclear Larmor frequency and the bar represents an ensemble average. At a certain orientation, the magnetization recovery originating from the pure phason or pure amplitudon relaxation mechanism should be either monoexponential or biexponential, depending on the ratio $W^{(1)}/W^{(2)}$, irrespective of where on the lineshape we measure it. If in the centre of the INC lineshape we obtain a monoexponential recovery, the same should hold everywhere on the absorption line, since the same EFG tensor elements contribute to relaxation. In our case we found in the middle of the spectrum a magnetization recovery that can be perfectly fitted by a single exponent (figure 9(*a*)). Thus at the chosen orientation one of the two transition probabilities $W^{(i)}$ is dominating the other or they are accidentally very close to each other. We can also define an effective spin–lattice relaxation time $T_{1\phi}$, which in this case (at

$T = -22\,^{\circ}\mathrm{C}$) is equal to $T_{1\phi} = 4.2$ ms. On figure 9(*b*), the magnetization recovery function of one of the two edge singularities is shown together with the attempt to fit it with a monoexponential function. The fit is obviously bad. This deviation from monoexponentiality does not come from the quadrupolar relaxation, since in that case it should be present also in the other parts of the INC spectrum. The observed non-monoexponentiality is introduced by the cross-relaxation mechanism, which tries to relax the edge singularities via the phason-relaxed part of the absorption line. This we can describe by writing two coupled equations for the relaxation of phason- and amplitudon-relaxed nuclei,

$$\mathrm{d}\langle I_z\rangle_\phi/\mathrm{d}t = -(1/T_{1\phi})(\langle I_z\rangle_\phi - I_{0\phi}) \tag{25a}$$

$$\frac{\mathrm{d}\langle I_z^n\rangle_A}{\mathrm{d}t} = \sum_k -\frac{1}{T_c^{kn}}(\langle I_z^k\rangle_\phi - I_{0\phi}^k) - \frac{1}{T_{1A}}(\langle I_z^n\rangle_A - I_{0A}^n) \tag{25b}$$

where $\langle I_z\rangle_\phi = \sum_i \langle I_z^i\rangle_\phi$ and index k runs over all phason-relaxed nuclei, to which an amplitudon-relaxed nucleus n is coupled in a cross-relaxation process. Here T_c^{kn} represents the cross-relaxation time for the transfer of longitudinal spin polarization from the phason-relaxed spin k to amplitudon-relaxed spin n. In equation (25*a*) we neglect the 'back' cross-relaxation since the phason relaxation mechanism is the dominant one. The amplitudon-relaxed nuclear spins see the phason-relaxed nuclei much like 'paramagnetic impurities'. The solution of equation (25*a*) is for the initial condition $\langle I_z(t=0)\rangle_\phi = -I_{0\phi}$ the standard relation

$$\langle I_z(t)\rangle_\phi = I_{0\phi}[1 - 2\exp(-t/T_{1\phi})]. \tag{26}$$

The solution of equation (25*b*) can be found with the *ansatz*

$$\langle I_z^n(t)\rangle_A - I_{0A}^n = [\langle I_z^n(0)\rangle_A - I_{0A}^n]\exp(-t/T_{1A})f(t). \tag{27}$$

When the initial condition is a complete inversion of both types of spins (of the same nuclear species) we get

$$\langle I_z^k(0)\rangle_\phi - I_{0\phi}^k = -2I_{0\phi}^k = -2I_0$$
$$\langle I_z^n(0)\rangle_A - I_{0A}^n = -2I_{0A}^n = -2I_0$$

out of which we find the initial condition $f(0) = 1$. The magnetization recovery function for $\langle I_z^n(t)\rangle_A$ becomes, dropping index n,

$$\frac{I_0 - \langle I_z(t)\rangle_A}{2I_0} = \exp(-t/T_{1A})\left[\left[1 + \sum_k \frac{1}{T_c^k}\Big/\left(\frac{1}{T_{1\phi}} - \frac{1}{T_{1A}}\right)\right.\right.$$
$$\left.\left.\times\left\{\exp\left[-t\left(\frac{1}{T_{1\phi}} - \frac{1}{T_{1A}}\right)\right] - 1\right\}\right]\right]. \tag{28}$$

From equation (28) we can get an approximate result for the initial part of the magnetization recovery function by expanding the term $\exp[-t(1/T_{1\phi} - 1/T_{1A})]$ in series and retaining the linear term only. Writing $\sum_k(1/T_c^k) = 1/T_c^{\mathrm{eff}}$ we get

$$(I_0 - \langle I_z(t)\rangle_A)/2I_0 = \exp(-t/T_{1A})(1 - t/T_c^{\mathrm{eff}}) \simeq \exp[-t(1/T_{1A} + 1/T_c^{\mathrm{eff}})]$$
$$\simeq \exp(-t/T_c^{\mathrm{eff}})$$

and the magnetization of the amplitudon-relaxed nuclei grows towards equilibrium with the effective cross-relaxation time T_c^{eff}, rather than with the amplitudon relaxation time T_{1A}. The magnetization recovery function of the edge singularities can be well fitted with equation (28) (figure 9(*c*)). The fitting parameter $T_c^{\text{eff}}/T_{1\phi} = 2.88$ agrees rather well with the experimentally determined total variation of T_1 over the lineshape, which is equal to 3. The other fitting parameter $T_{1A}/T_{1\phi}$ does not affect the fit much and is thus determined rather imprecisely as a factor of around 10. This might also be affected by the repetition time of the pulse sequence, since for precise measurements one should repeat the sequence after as many as around 100 times the longest time constant of relaxation, for a proper thermal equilibrium to be reached, before a new sequence starts. It is interesting to compare the above results to the results on pure ^{35}Cl nuclear quadrupole resonance (NQR) (Chen and Ailion 1989, Milia and Papavassiliou 1989). There they have shown that in the INC phase $T_{1\phi}$ is temperature-independent, whereas T_{1A} is temperature-dependent, but its dependence on temperature is weaker than the theoretically expected $T_{1A} \propto \Delta_A \propto (T_I - T)^{1/2}$ and does not smoothly match the T_1 value in the commensurate phase at the lock-in transition at T_c. There it exhibits a jump of a factor of about 3 in a narrow temperature interval. Close to T_c the ratio $T_{1A}/T_{1\phi}$ amounts to a factor 14, which is larger than in the ^{87}Rb case shown in this paper. In the case of ^{35}Cl NQR cross-relaxation (due to its dipolar origin) should be less effective than in the ^{87}Rb case since the cross-relaxation rate is proportional to the square of the dipolar coupling constant, and thus to the fourth power of the nuclear magnetic moment. The gyromagnetic ratio of the ^{35}Cl nucleus is 3.3 times smaller than that of the ^{87}Rb nucleus, which would make the cross-relaxation rate smaller by a factor of about 120. This is, in our opinion, the reason for a stronger temperature dependence of T_{1A} in the ^{35}Cl NQR case.

4. Conclusions

We have shown that a 2D spin–lattice relaxation technique allows for a precise determination of a variation of the spin–lattice relaxation time over the inhomogeneously broadened incommensurate lineshape. In the middle of the lineshape, we obtain the phason relaxation time, whereas the edge singularities, which should be relaxed by amplitudons, are relaxed via a cross-relaxation process to the phason-relaxed part of the spectrum. This process bypasses—except close to T_I—the amplitudon relaxation mechanism. This explains the fact that the relaxation time of the edge singularities follows the temperature behaviour of $T_{1\phi}$. The experimentally obtained value for the total variation of T_1 over the lineshape, which is a factor of 3.01, agrees well with that obtained from a theoretical model for the cross-relaxation between amplitudon- and phason-relaxed parts of the spectrum, which yields a factor of 2.88.

We are now able to make a more precise estimate of the phason gap Δ_ϕ, which was in our earlier paper (Blinc *et al* 1985a) determined from ^{87}Rb NMR in Rb_2ZnCl_4 from the ratio

$$T_{1\phi}/T_{1A} = \Delta_\phi/\Delta_A.$$

There we have used an independently determined amplitudon gap Δ_A (Petzelt 1981) and obtained from the measured values of $T_{1\phi}$ and T_{1A} an estimate for Δ_ϕ as 10^{11}–10^{12} s^{-1}. As it now turns out, T_{1A} was in fact not properly determined in view of

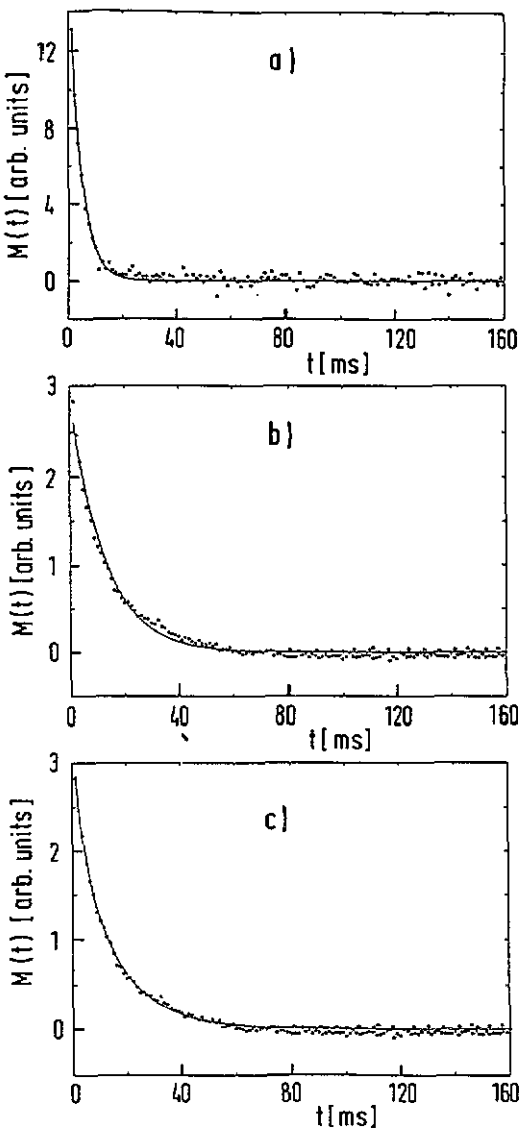

Figure 9. Magnetization recovery curve $M(t)$ of ^{87}Rb $1/2 \rightarrow -1/2$ transition in the incommensurate phase of Rb_2ZnCl_4 at $T = -22$ °C. Dots represent experimental points and the full curve is a fitted curve. (*a*) $M(t)$ taken at the centre of the inhomogeneously broadened NMR lineshape, where the relaxation is caused by the phason fluctuations. The full curve represents a fit with a monoexponential function $\exp(-t/T_{1\phi})$ ($T_{1\phi} = 4.2$ ms). (*b*) $M(t)$ taken at one of the two edge singularities together with the attempt to fit it with a monoexponential function of the form $\exp(-t/T_1)$. The fit is not good. (*c*) The same magnetization recovery function as in (*b*), but fitted with equation (28). The fit is now good with $T_c^{\text{eff}}/T_{1\phi} = 2.88$.

the cross-relaxation process T_c^{eff}. Since we have shown in this paper that the real T_{1A} is about four times longer than T_c^{eff}, we now get a corrected estimation for the phason gap to lie in the range $\Delta_\phi \simeq 10^{10}$–$10^{11}$ s^{-1}. The correction factor and the effectiveness of the cross-relaxation process are of course different for different nuclei with different magnetic moments and different crystal structures. For ^{87}Rb the effects are much larger than for ^{39}K or ^{35}Cl. This also explains the fact that smaller phason gaps were determined from ^{35}Cl than from ^{87}Rb T_1 data in the same crystal.

References

Abragam A 1961 *The Principles of Nuclear Magnetism* (Oxford: Clarendon) p 412

Blinc R 1981 *Phys. Rep.* **79** 331
Blinc R, Ailion D C, Dolinšek J and Žumer S 1985a *Phys. Rev. Lett.* **54** 79
Blinc R, Dolinšek J, Prelovšek P and Hamano K 1986 *Phys. Rev. Lett.* **56** 2387
Blinc R, Seliger J and Žumer S 1985b *J. Phys. C: Solid State Phys.* **18** 2313
Bodenhausen G, Vold R L and Vold R R 1980 *J. Magn. Reson.* **37** 93
Bruce A D 1980 *J. Phys. C: Solid State Phys.* **13** 4615
Bruce A D and Cowley R A 1978 *J. Phys. C: Solid State Phys.* **11** 3609
Chen S and Ailion D C 1989 *Solid State Commun.* **69** 1041
Dolinšek J 1991 *J. Magn. Reson.* **92** 312
Hoult D I and Richards R E 1975 *Proc. R. Soc.* A **344** 311
Milia F and Papavassiliou G 1989 *Phys. Rev.* B **39** 4467
Millhauser G L and Freed J H 1984 *J. Chem. Phys.* **81** 37
Müller K, Wassmer K H and Kothe G 1990 *Advances in Polymer Sciences* vol 95 (Berlin: Springer)
Petzelt J 1981 *Phase Transitions* **2** 155
Schleicher A, Müller K and Kothe G 1989 *Liq. Cryst.* **6** 489
—— 1990 *J. Chem. Phys.* **92** 6432
Slichter C P 1980 *Principles of Magnetic Resonance* (Berlin: Springer) ch 5
Žumer S and Blinc R 1981 *J. Phys. C: Solid State Phys.* **14** 465